



Title	Basic Studies on Plasma Sprayed Ceramics Coatings (Report 1) : Erosion Mechanism at ACT-JP Process(Materials, Metallurgy & Weldability)
Author(s)	Arata, Yoshiaki; Ohmori, Akira; LI, Chang-Jiu
Citation	Transactions of JWRI. 1986, 15(2), p. 339-348
Version Type	VoR
URL	https://doi.org/10.18910/4648
rights	
Note	

The University of Osaka Institutional Knowledge Archive : OUKA

<https://ir.library.osaka-u.ac.jp/>

The University of Osaka

Basic Studies on Plasma Sprayed Ceramics Coatings (Report 1)[†]

— Erosion Mechanism at ACT-JP Process —

Yoshiaki ARATA*, Akira OHMORI** and Chang-Jiu LI***

Abstract

The erosion mechanism of ceramics coatings in Arata Coating Test with Jet Particles (ACT-JP) process was investigated experimentally and theoretically based on a fatigue crack propagation model by utilizing the relation between the erosion rate and ACT-JP condition. As results, the erosion of ceramics coatings depends on the crack propagation due to repetitive impact of jet particles and the separation of flattened ceramics particles from coating along the interface between ceramics particles. The erosion rate of ceramics coatings depends on the bonding strength of ceramics coating. It is possible to evaluate the bonding strength of ceramics coatings by measuring the erosion rate in ACT-JP process.

KEY WORDS: (Arata Coating Test) (Erosion Mechanism) (Ceramics Coating) (Flattened Ceramics Particles) (Erosion Rate) (Jet Particles)

1. Introduction

The plasma sprayed ceramics coating is made of flattened ceramics particles in which there exists much unadhesive area presented as porosity. The properties of ceramics coatings such as wear-resistance, heat-resistance, corrosion-resistance etc. will be greatly effected by many factors such as bonding strength between the flattened ceramics particles and porosity. The mechanical properties of ceramics coatings depend on bonding strength of ceramics particles, which determine the working life of coatings used at high stressed parts. With the increase of requirements of wide application in various severe environments, the ceramics coatings with high quality are demanded. However, at present, it is much difficult to evaluate precisely the mechanical properties of ceramics coatings because of porosity in it. Therefore, it is necessary to develop the testing method to evaluate effectively the mechanical properties of ceramics coatings.

At present, the testing methods used conventionally for ceramics coatings are metallographic examination, hardness tests and estimation of adhesion and tensile strength. For the mechanical properties of ceramics coatings, the tensile strength and hardness test of these coatings are usually carried out. For testing of tensile strength for the coatings with porosity, the scatter presented in the test results obtained is often so large that the tensile strength can not be used as an effective criterion to evaluate the bonding strength of ceramics coatings.¹⁾ The micro-hardness, because it is much easy to measure, is a commonly quoted parameter for ceramics coatings. But

the hardness of coatings is also largely effected by the porosity and reading error.²⁾ For unhomogenous ceramics coating, it was reported that its mechanical properties would be effectively evaluated by erosion test using a stream of jet particles which are accelerated with compressed air to get certain kinetic energy and then impact the coating.^{1,3)}

At present paper, the erosion mechanism of ceramics coating at ACT-JP process will be discussed. It will be evidenced that it is possible to evaluate the bonding strength of ceramics coating using ACT-JP method.

2. Materials and Experimental Procedures

Five kinds of oxide ceramics powders of $\text{Al}_2\text{O}_3\text{-TiO}_2$ system and one of ZrO_2 stabilized by Y_2O_3 were used in plasma spraying which have the same grain size distribution. Their chemical compositions are shown in Table 1.

The ceramics coatings were obtained by plasma spraying. Table 2 shows the spraying conditions.

The principle of ACT-JP method is schematically shown in Fig. 1. For ACT-JP test, a stream of jet particles are accelerated with precisely controlled compressed air stream to get certain kinetic energy and made impact the ceramics coating at a given jet angle. Then the erosion of ceramics coating occurs. The jet angle can be adjusted. The weight loss of ceramics coating after ACT-JP test was measured with the precise balance by which it can be readable until 0.01 mg. The conditions of ACT-JP test used are shown in Table 3. The jet particles used in this

† Received on November 5, 1986

* Professor

** Associate Professor

*** Graduate Student

Transactions of JWRI is published by Welding Research Institute of Osaka University, Ibaraki, Osaka 567, Japan

Table 1 Chemical compositions of powders used for spraying.

Materials	Chemical compositions (wt%)			
	Al ₂ O ₃	TiO ₂	ZrO ₂	Y ₂ O ₃
Al ₂ O ₃	100	—	—	—
2.3%TiO ₂	97.7	2.3	—	—
13%TiO ₂	87	13	—	—
40%TiO ₂	60	40	—	—
TiO ₂	—	100	—	—
ZrO ₂	—	—	92	8

Table 2 Plasma spraying conditions.

Spraying apparatus	Plasmadyne (Mach 1)
Plasma gas (Ar)	4.2 kg/cm ²
Auxiliary gas (He)	4.2 kg/cm ²
Powder carrier gas (Ar)	5.6 kg/cm ²
Hopper setting	3.5~4.0 rpm
Spraying current	800 A
Spraying voltage	35 V
Spraying distance	100 mm
Cooling air pressure	1 kg/cm ²

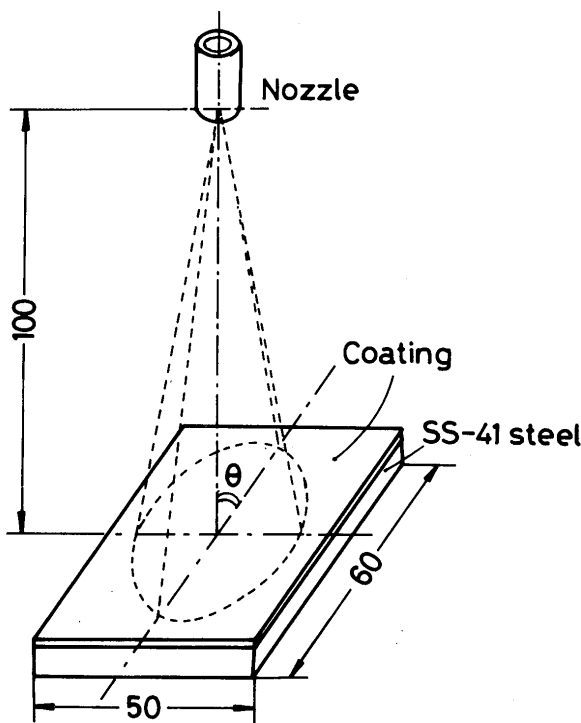


Fig. 1 Schematic diagram of ACT-JP test.

study were 60 mesh alumina powders (Showa Denko 41 Morandamu) and the grain size was between 250 and 420 μm . Figure 2 shows its SEM micrograph.

The surface of ceramics coating was investigated with SEM and Surfcoorder after ACT-JP test.

Table 3 Conditions of ACT-JP test.

Nozzle diameter	5.2 mm
Abrasive	60 mesh fused Alumina powders
Air pressure	5 kg/cm ²
Air flow rate	370 l/min
Abrasive carrier air flow rate	50 l/min
Jet angle	35~90°
Jet distance	100 mm

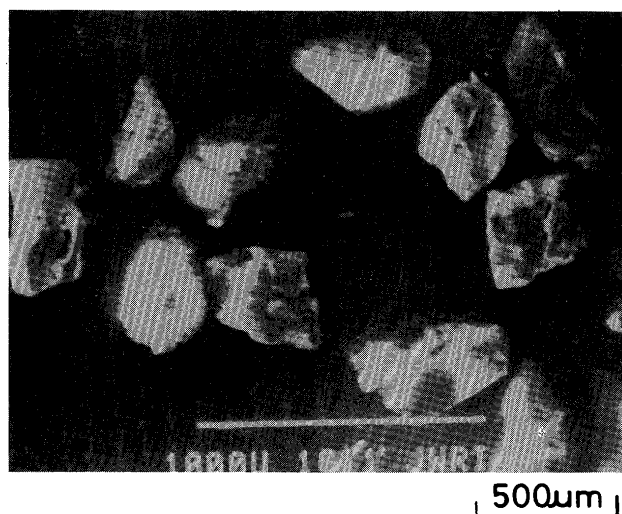


Fig. 2 SEM photograph of Alumina powders used as abrasives.

3. Experimental Results and Discussion

3.1 Initial erosion behavior of ceramics coatings at ACT-JP process

In order to know the effect of surface condition on the erosion behavior, two kinds of samples with different surface conditions were used. One was as sprayed, and the other was surface polished with emery paper to 1000#. Each sample was tested at jet angle of both 35 and 90 degree. Figure 3 shows the relation between weight loss and weight of abrasives for TiO₂ coatings with different surface conditions at jet angle of 90 degree. The erosion rate represented as ratio of weight loss of coatings to weight of abrasives is also shown in Fig. 3 as the function of the weight of abrasives. As shown, the weight loss of ceramics coatings increases with the increase of the weight of abrasives and for the sample as coated the erosion rate is almost constant. But for the sample with polished surface the erosion rate is lower than that of as coated one at initial state and increases with the weight of abrasives to reach the value for as coated sample. Figure 4 shows the change of surface profiles of polished sample with the weight of abrasives. Figure 5 (a) shows the roughness curve of as sprayed surface and (b), (c) show those of the same surface as shown in Fig. 4 (e) and (f) respectively.

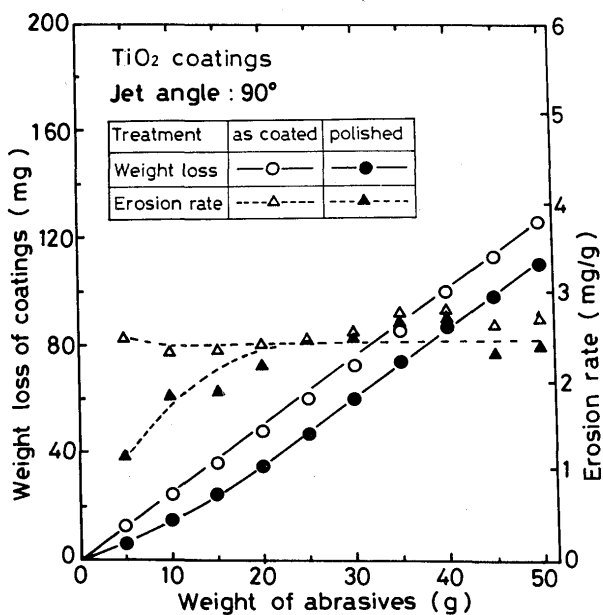


Fig. 3 Effect of surface treatments of ceramics coatings on the ACT-JP results at jet angle of 90 degree.

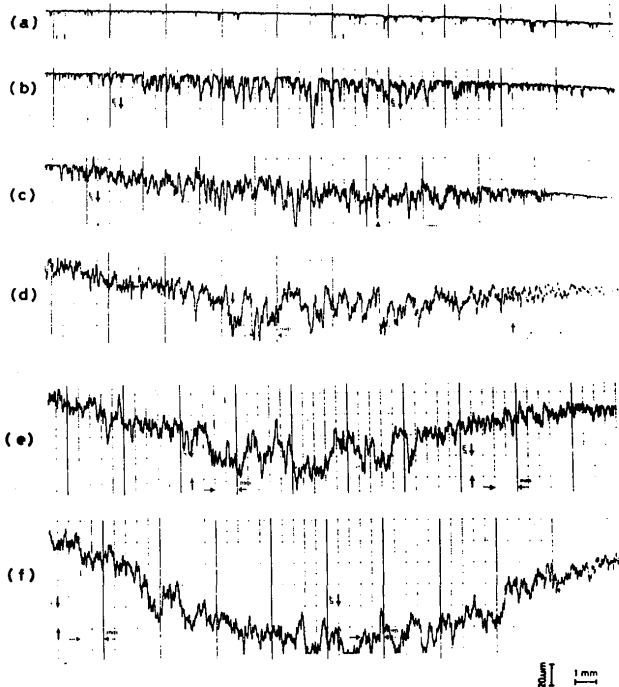


Fig. 4 Change of TiO₂ coating surface with weight of abrasives during ACT-JP test: (a) polished original surface, (b) 5g, (c) 15g, (d) 20g, (e) 30g and (f) 50g.

It is clear that when the erosion rate of sample with polished surface becomes equal to that of the sample with as coated surface, the surface state of two kinds of samples reaches the same. This state is called the steady erosion state in our studies. With regard to this state, the state where the erosion rate was influenced greatly by surface condition is called initial erosion state.

Figure 6 shows the relation between the weight of abrasives and weight loss and erosion rate for TiO₂ coat-

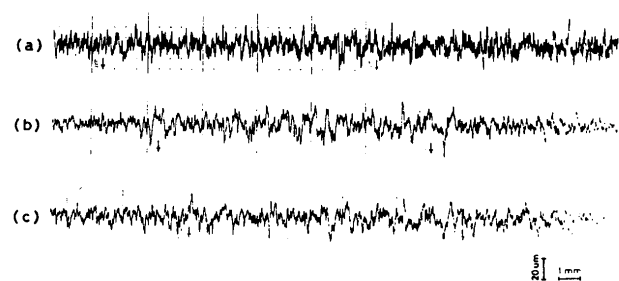


Fig. 5 Surface roughness curves of TiO₂ coatings: (a) as sprayed surface, (b) the same surface as Fig. 4 (e), (c) the same surface as Fig. 4 (f).

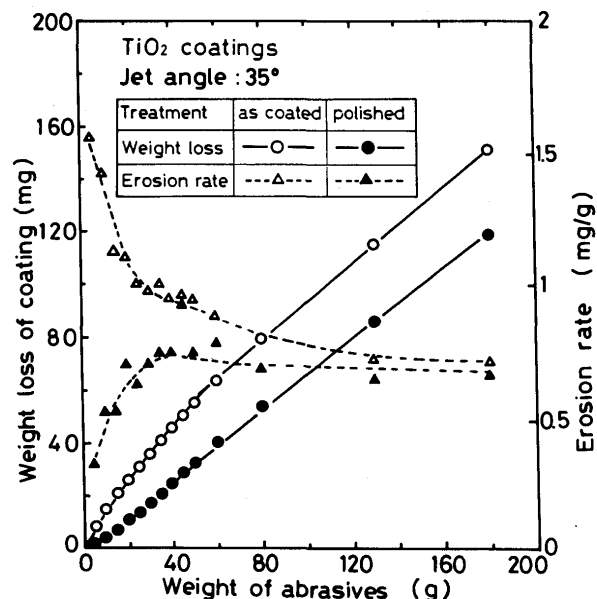


Fig. 6 Effect of surface treatment of ceramics coatings on the ACT-JP results at jet angle of 35 degree.

ings with two different surface conditions at jet angle of 35 degree. It also can be recognized that the erosion of ceramics coatings can be divided into initial erosion state and steady erosion state. Although the erosion rate changed greatly at different tendency for two kinds of surface conditions at initial state, it almost became the same at steady erosion state. It is considered that the erosion rate at steady erosion state indicates the certain mechanical properties of ceramics coating itself.

Based on above results, it was found that although the weight of abrasives to be necessary for ceramics coatings to reach the steady erosion state was different and decreased with increase of jet angle, it was sufficient to make the surface reach a steady erosion state using 20g abrasives as jet material at beginning of test in our studies.

3.2 Erosion of ceramics coatings at steady erosion state

Figure 7 shows the relation between weight loss and the weight of abrasives at the steady erosion state for four kinds of ceramics coatings at different angles from 35 to 90 degree. As shown, the weight loss of ceramics coatings

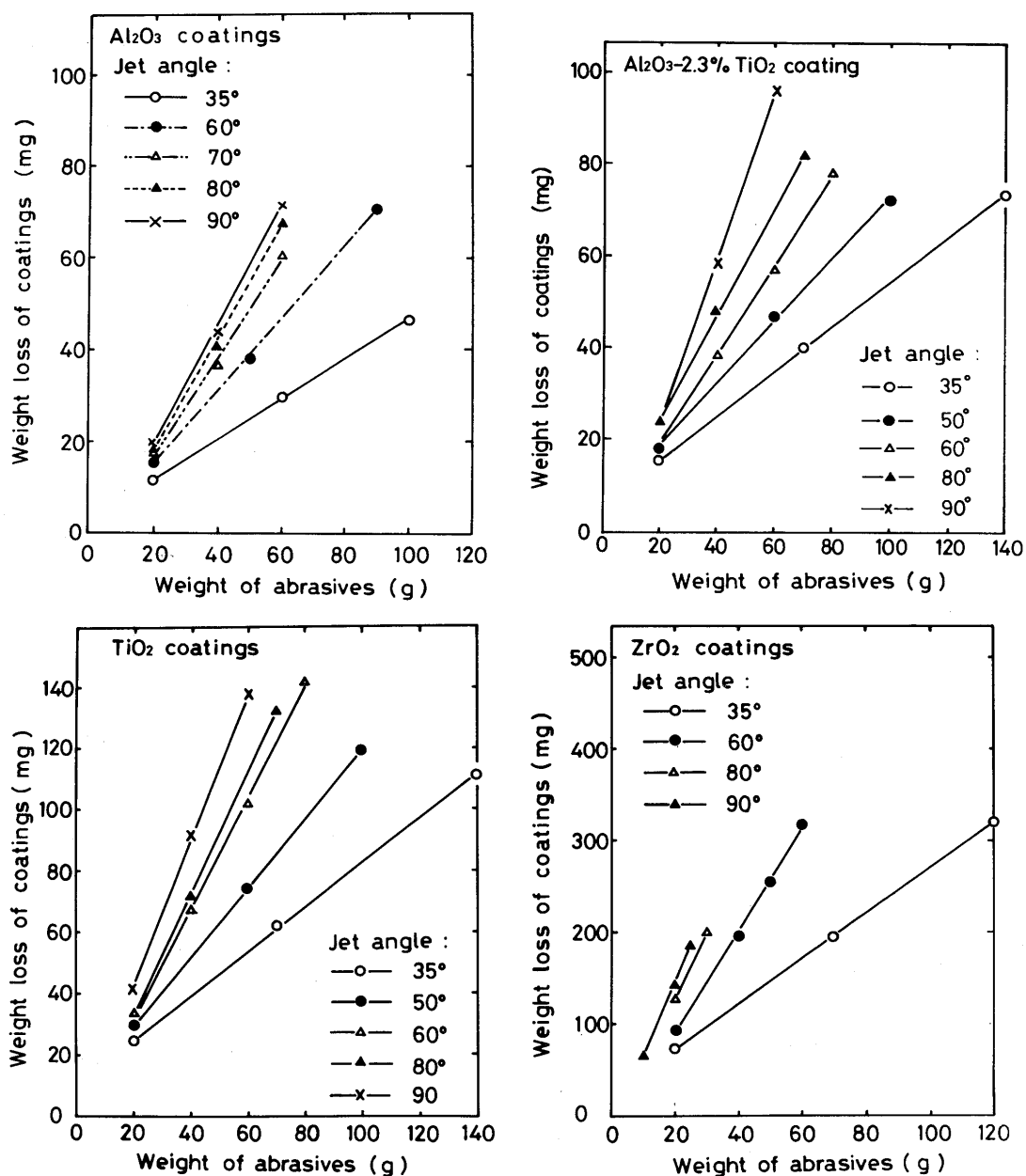


Fig. 7 Relation between weight loss of coatings and weight of abrasives at steady erosion state of ACT-JP test for various ceramics coatings.

increased linearly with the increase of the weight of abrasives at the certain jet angle. That is, the erosion rate at a certain jet angle was definitely defined at the steady erosion state. It was also noted that the erosion rate increased with the increase of jet angle.

3.3 Erosion mechanism of ceramics coatings at ACT-JP process

Figure 8 shows the surface roughness before and after ACT-JP test for 40%TiO₂ and Al₂O₃ ceramics coatings. As mentioned before, it was noticed that the roughness of coating surface almost shows no changes after the test, compared with that of as coated one. It was considered

that this is because the ceramics coatings weared out as a particle one after another from the interface between the flattened ceramics particles when it was impacted by such a stream of jet particles. Therefore, the surface newly presented after ACT-JP test is constrained only by the flattened state. This state depends on the spraying conditions for given spraying ceramics when the fused ceramics particles during spraying impacted on the substrate or coating already formed. Figure 9 shows the SEM structures of as coated surface for 40%TiO₂ ceramics coating. It was observed that ceramics coating is made of flattened ceramics particles. The typical size of flattened particles was also illustrated. Figure 10 shows the typical SEM

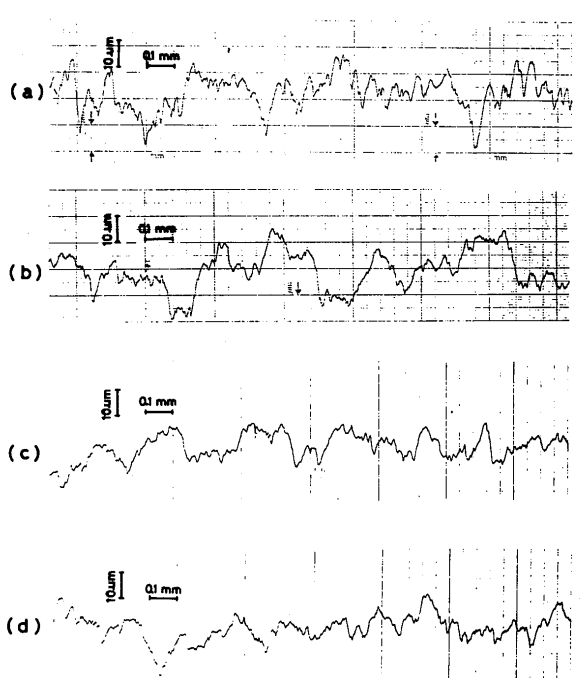


Fig. 8 Comparison of surface roughness of ceramics coatings (cut-off of waveness: 0.8 mm): (a) and (b) are roughness curves before and after ACT-JP test for 40% TiO_2 coatings, (c) and (d) are those before and after ACT-JP test for Al_2O_3 coating respectively.

structures of surface after ACT-JP test for 40% TiO_2 ceramics coating. The structures of areas of A, B, C in Fig. 10 (a) are further magnified and are shown in Fig. 10 (b) (c) (d) respectively. Comparing with Fig. 9, it is clear that craters presented at A and B parts in Fig. 10 where flattened ceramics particles were removed during ACT-JP test and at C parts a flattened ceramics particle remained without separating from bulk coating. As shown in those SEM photographs, the distinct crack was not observed to appear at the surface impacted by jet particles. But when the ACT-JP test was carried out on the cross section of coating, it was observed that it is preferred for cracks to form along the interface between flattened ceramics particles. As a illustration, Fig. 11 shows the typical cracks induced through the testing of micro Vickers hardness at cross section of ceramics coatings. It is obvious that the cracks were prefered to form and propagate along the interface between flattened ceramics particles. Therefore, from above results, it can be considered that the erosion of ceramics coating at ACT-JP process results from the separating of flattened ceramics particles. This is due to forming and propagating of the cracks along interface between flattened ceramics particles which are resulted from repetitive impacts of the stream of jet particles.

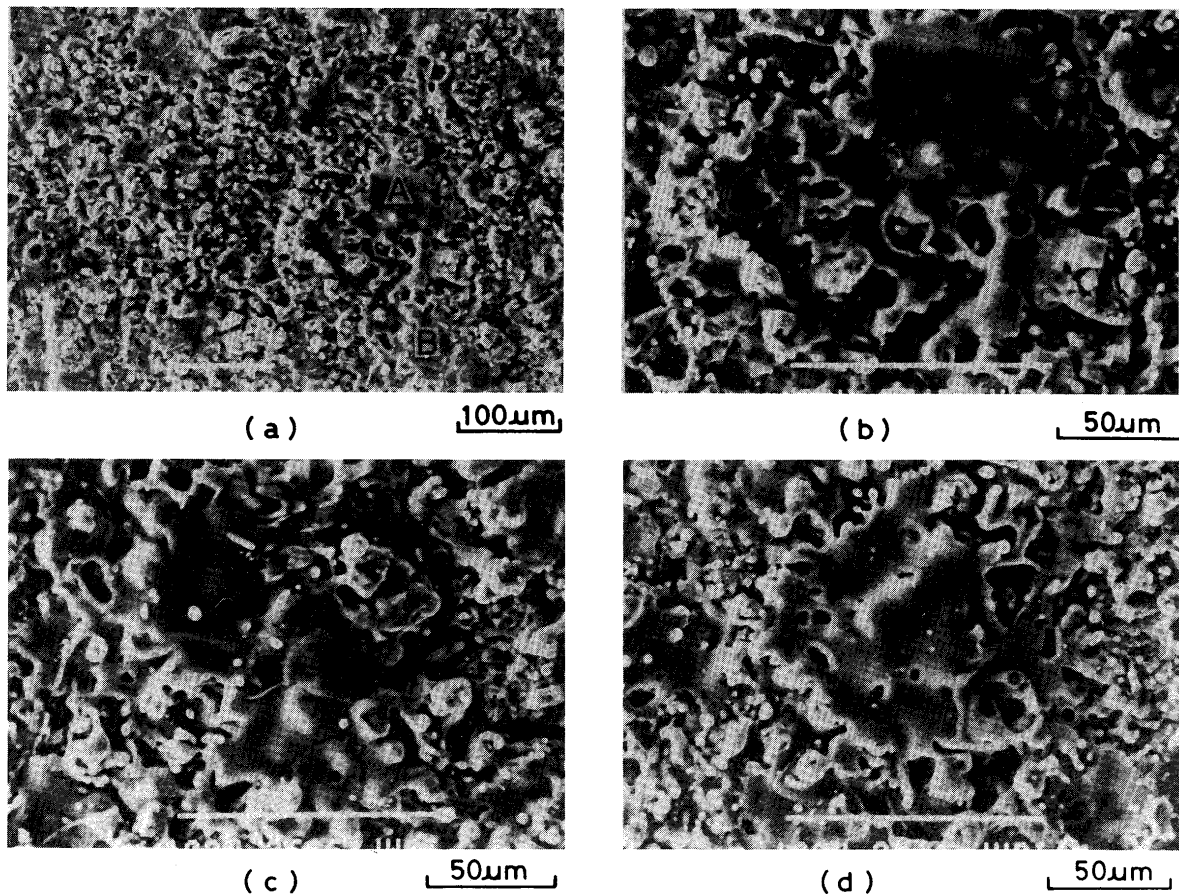


Fig. 9 SEM photographs of as sprayed coating surface of 40% TiO_2 ceramics: (b) and (c) are areas A and B in (a) respectively.

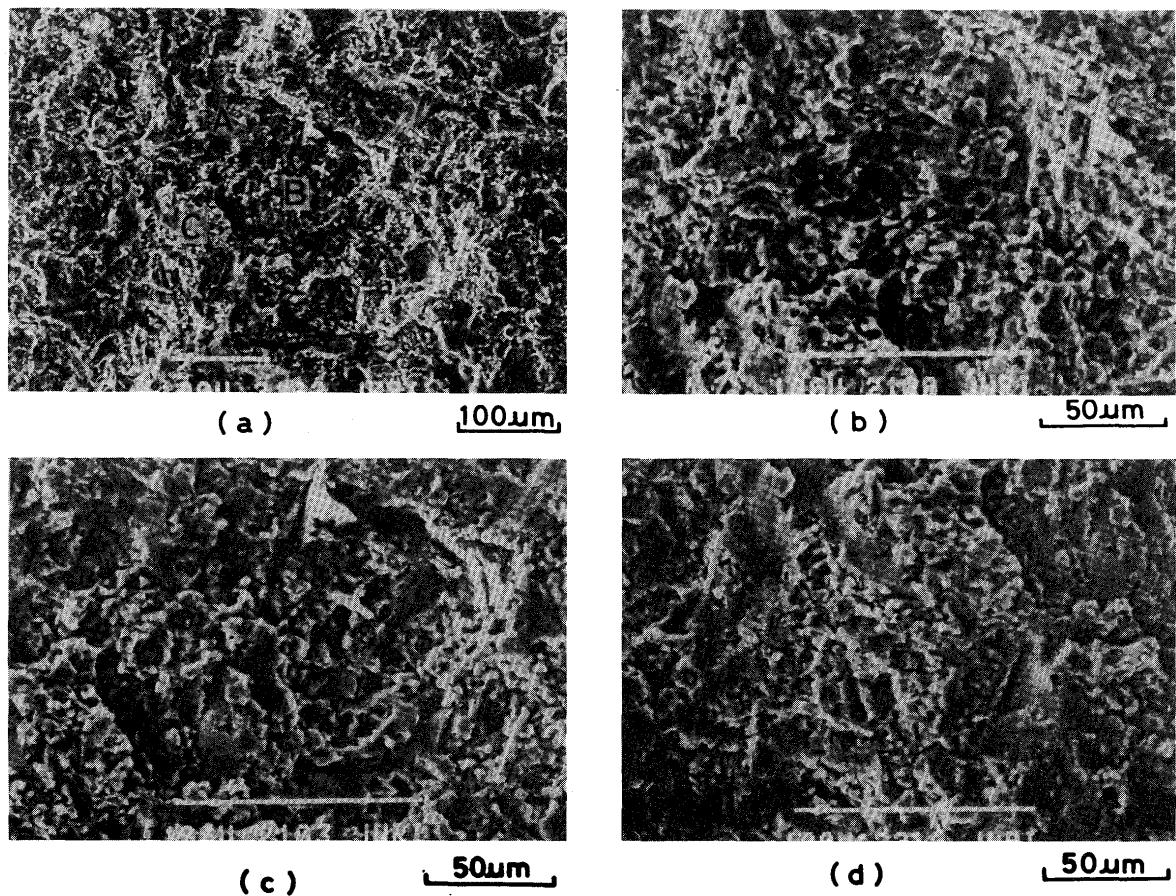


Fig. 10 SEM photographs of 40% TiO_2 coating surface after ACT-JP test; (b), (c) and (d) are areas A, B, C in (a) respectively.

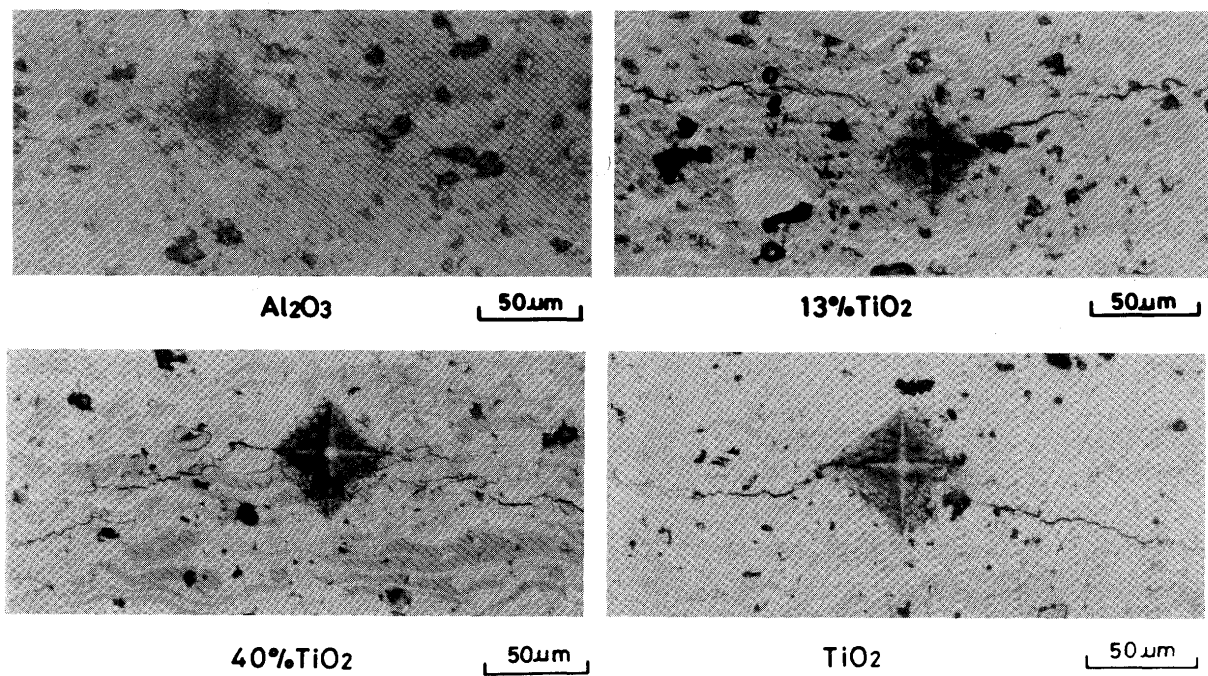


Fig. 11 Typical microphotographs of cracks induced at cross-section of ceramics coatings by measuring micro-hardness (load: 1 kgf; load time: 30 sec).

3.4 Theoretical analysis of erosion mechanism

The erosion of materials shows different characteristics in dependency of erosion rate on jet angle when they are impacted with a stream of jet particles, whether the materials are brittle or ductile. This results from two forms of erosion mechanism.⁴⁾ For brittle materials, the predominant mechanism is the cracking of surface and subsurface with subsequent intersection of cracks and then material removes, which depends on the normal component of impact force with respect to the surface. For the ductile materials, both deformation wear and cutting wear all act on simultaneously. The former is associated with normal component of impact force and later is associated with the parallel one to the surface impacted. For brittle ceramics coatings, the experimental results confirm that the erosion results from the separating of ceramics particles due to the forming and propagating of cracks along the interface between ceramics particles. For simplicity, it is considered that two components of impact force of jet particle contribute to cracking and propagating of cracks although they play different roles at ACT-JP process as mentioned later. At steady erosion stage, the propagating of cracks dominates the erosion rate.

Figure 12 shows schematically the structure of ceramics coating and interaction between the coating and jet particles when they impact on ceramics coating at jet angle of θ degree. The repetitive impact of jet particles equates with a repetitive force which acts on the ceramics coating. F is the impact force generated when a jet particle is brought into contact with ceramics coating. $F \sin\theta$ and $F \cos\theta$ are normal and parallel components of impact force with respect to coating surface respectively. The cracks which initiate from unbonding areas such as porosity gradually propagate along the interface under repetitive action of impact force and the ceramics particles separate from coating. For the materials on which the force repetitively acts, the fatigue fracture occurs. When

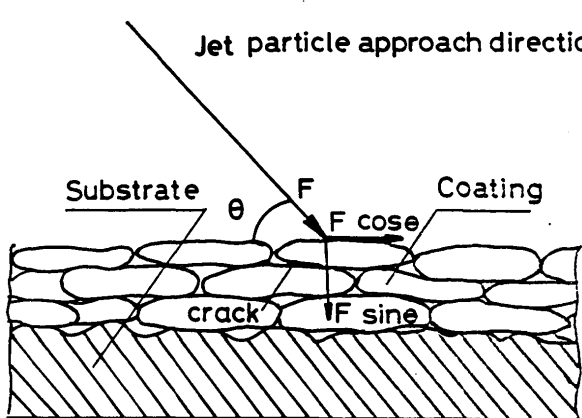


Fig. 12 Schematic diagram of cross-section structure of coating and interaction between coating and jet particle.

the precursory cracks exist in materials, the fracture depends on the propagation rate of crack. Generally, propagation rate of fatigue crack depends on the force and size of the crack. It may be adapted to the erosion at steady erosion state of ACT-JP test. Therefore, the propagation rate of crack at steady erosion state can be expressed as following.

$$\frac{dS}{dN} = K_a F_{eff}^n S^{n/2} \quad (1)$$

where S is fractured cross-section area (cm^2), expressing the size of crack; N is jet particle number; dS/dN is the propagation rate of the crack; n is the coating constant; K_a is the ACT-JP constant. F_{eff} is effective impact force to propagation of crack and the normal and parallel components of impact force F are considered according to the roles they play in ACT-JP test, which are expressed as $(1 - \gamma)$ and γ for two components respectively, it is given by Eq. (2).

$$F_{eff} = F ((1 - \gamma) \sin\theta + \gamma \cos\theta) \quad 0 \leq \gamma \leq 1 \quad (2)$$

where γ is the coating fracture coefficient. The impact force F is function of contact time during the impact according to Hertz impact theory. However, the impact wear depends heavily on maximum impact force.⁵⁾ For simplicity, F is supposed to be the maximum impact force of a jet particle in our studies.

Here S° is the apparent adhesive area of one flattened ceramics particle and S_o is the initial crack size from which the crack propagates into the steady erosion state. The separating condition for ceramics particle due to the impact of jet particles is given by Eq. (3).

$$S_{max} > S^\circ - F \cos\theta / \tau \quad (3)$$

where τ is shear strength of ceramics particles. When the size of crack exceeds S_{max} , the ceramics particles separate from coating.

Therefore, the jet particle number N required to separate one single ceramics particle of coating can be calculated as follow.

$$N = \frac{1}{K_a} \int_{S_o}^{S_{max}} \frac{ds}{F_{eff}^n S^{n/2}} \\ = \frac{2}{K_a F_{eff}^n (n-2)} \left\{ \left(\frac{1}{S_o}\right)^{\frac{(n-2)}{2}} - \left(\frac{1}{S_{max}}\right)^{\frac{(n-2)}{2}} \right\} \quad (4)$$

If $\beta = (2-n)/2$ and $S^* = S_o/S^\circ$ then N is expressed in following form.

$$N = - \frac{S^{\circ\beta}}{\beta K_a F_{eff}^n} \left\{ S^{*\beta} - \left(\frac{S_{max}}{S^\circ}\right)^\beta \right\} \quad (5)$$

Thus, the erosion rate M^* is obtained:

$$M^* = v_c \rho_c / v_b \rho_b N$$

Where ρ_c and v_c are specific density and average volume of a single spraying powder respectively and ρ_b and v_b are those of a single jet particle. By expressing the mass ratio of flattened ceramics particle to a jet particle as m^*

$$m^* = v_c \rho_c / v_b \rho_b \quad (7)$$

The erosion rate becomes

$$M^* = m^* / N \quad (8)$$

The Eqs. (3) and (5) are substituted into Eq. (8), and finally the erosion rate can be obtained:

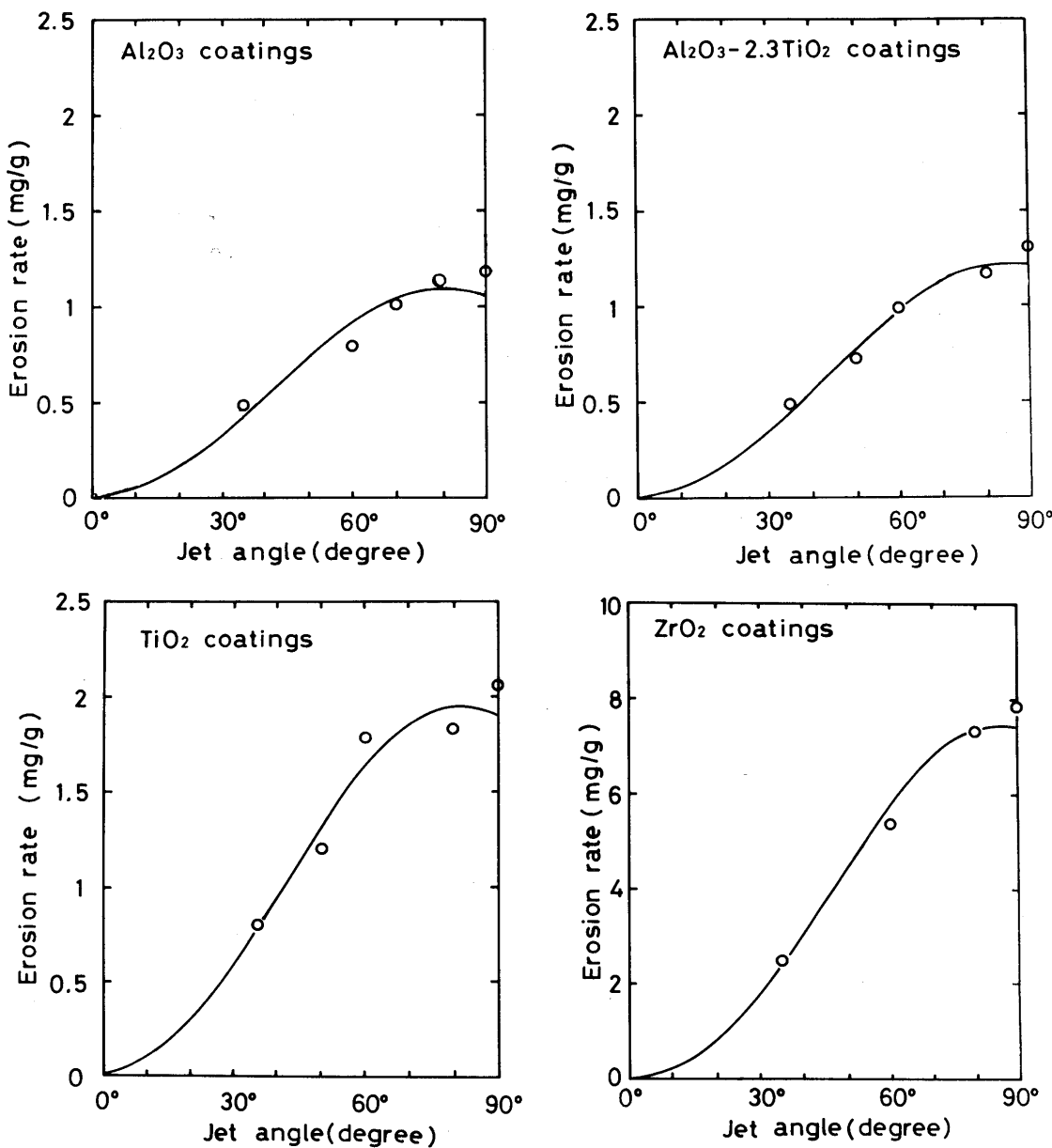


Fig. 13 Relation between erosion rate and jet angle for various coatings (○ measured; — calculated).

function of jet angle only,

$$C = - \frac{m^* \beta K_a F^n}{S^* \beta} \quad (10)$$

can be considered as a constant. Then the constants γ , n and S^* which only depend on coating and α_f as well were determined by simulation. **Figure 13** shows the relation between erosion rate and jet angle. It was recognized that the theoretical value is well consistent with experimental data. From these constants, it was found that bonding constant α_f was less than 0.001 for each coating and so that it could be neglected. This may be because the fracture of brittle ceramics coatings depends on tensile stress rather than shear stress of coating.

From Hertz impact theory, when a jet particle impacts on the coating at a jet particle velocity V perpendicularly, the maximum impact force F is

$$F = \frac{C_0}{C_1} m^{3/5} R^{1/5} V^{6/5} \quad (11)$$

where

$$C_0 = (5/4)^{3/5} (4/3\pi)^{2/5}$$

$$C_1 = \left(\frac{1 - \nu_1^2}{\pi E_1} + \frac{1 - \nu_2^2}{\pi E_2} \right)^{2/5}$$

E_1 and E_2 are Young's modulus of jet particle and coating respectively and likewise ν_1 and ν_2 the Poisson's ratio. m and R are the mass and effective radius of jet particles. The maximum impact force can not be obtained exactly from Eq. (11), because the material constants are unknown. But it is noticed that the relative maximum impact force is only the function of the relative velocity of jet particles for the given jet particles and coating.

$$F^* = V^{*6/5} \quad (12)$$

where F^* and V^* are relative maximum impact force and relative velocity of jet particles.

Meanwhile, from Eq. (9), the relative maximum impact force can also be obtained from erosion rate for a given coating and certain ACT-JP condition except the velocity of jet particles which is changed through the change of compressed air flow rate.

$$F_{ij}^* = F_i / F_j = \sqrt[6]{M_{i,j}^* / M_j^*} \quad (13)$$

Where F_i and M_i^* are maximum impact force and erosion rate at a jet particle velocity V_i before it impacts on the coating and likewise the subscript j .

The velocity of jet particles with average grain size was calculated from one dimensional model⁵⁾ at different air flow rate. The results obtained are shown in **Table 4**. The relative maximum impact force was calculated from erosion rate according to Eq. (13) at different air flow rate.

Table 4 Calculated jet particle velocity at various air flow rates.

Air flow rate (l/min)	250	300	370
Air velocity (m/sec)	235	275	330
Jet particle velocity (m/sec)	46	53	62
Relative jet particle velocity	1.00	1.15	1.35

The relation between relative jet particle velocity and relative maximum impact force is shown in **Fig. 14** for three kinds of ceramics coatings. For comparison, the result based on Hertz impact theory is also shown in Fig. 14. From this figure, the good consistency between the theoretical result obtained from Hertz impact theory and those calculated according to the erosion rate expressed with Eq. (9) were recognized.

The above results provide the justification of Eq. (9) for estimation of erosion rate derived on the basis of the propagation of cracks along the interface of flattened ceramics particles due to repetitive impact of jet particles. Thus this further confirms the erosion mechanism at ACT-JP process.

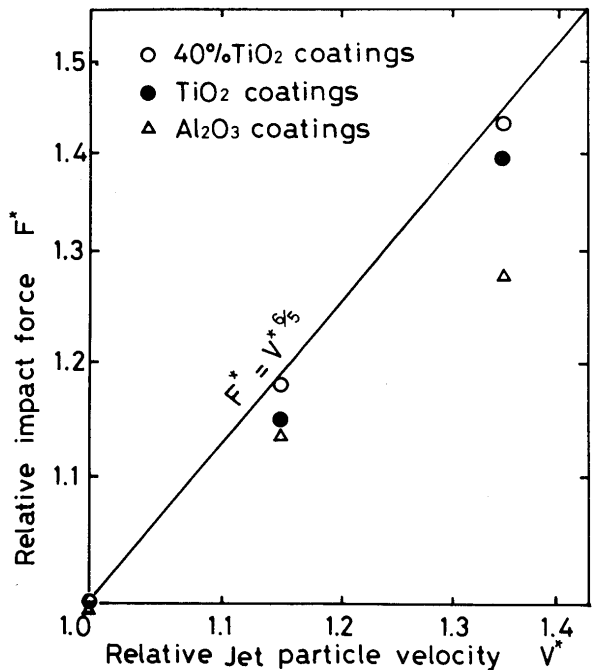


Fig. 14 Relation between relative impact force and relative jet particle velocity.

4. Conclusions

From the results obtained, it is clear that the erosion of ceramics coatings in ACT-JP process depends on propagation of cracks along the interface between the flattened ceramics particles which is brought out by repetitive impacts of jet particles, and subsequent separation of ceramics particles from the coating. The erosion rate at steady erosion state of ACT-JP test expresses the bonding

strength of ceramics particles from which it is possible to evaluate the bonding strength of ceramics coatings.

Acknowledgement

The authors would like to express their thanks to Mr. R. Nagayama for his cooperation in the experiments.

References

- 1) Y. Mima, M. Uemura: J. Thermal Spraying Society of Japan, Vol. 8 No. 1 (1971) 8 (In Japanese).
- 2) M. Kishida, J. High Temperature Society of Japan, Vol. 10, Supplement (1984) 230 (In Japanese).
- 3) Y. Mima, J. Thermal Spraying Society of Japan, Vol. 8 No. 2 (1971) 1 (In Japanese).
- 4) J. H. Neillson and A. Gilchrist, Wear, Vol. 2 (1968) 111.
- 5) P. A. Engel, "Impact Wear of Materials", Elsevier Scientific Publishing Company, Amsterdam Oxford New York (1976).